Supplemental Materials For:

ZNF397 Deficiency Triggers TET2-driven Lineage Plasticity and AR-Targeted Therapy Resistance in Prostate Cancer

Yaru Xu[1], Yuqiu Yang[2], Zhaoning Wang[1,3], Martin Sjöström[4], Yuyin Jiang[1], Yitao Tang[5], Siyuan Cheng[6], Su Deng[1], Choushi Wang[1], Julisa Gonzalez[1], Nickolas A. Johnson[1], Xiang Li[1], Xiaoling Li[1], Lauren A Metang[1], Atreyi Mukherji[1], Quanhui Xu[1], Carla Rodriguez Tirado[1], Garrett Wainwright[1], Xinzhe Yu[7], Spencer Barnes[8], Mia Hofstad[9], Yu Chen[10], Hong Zhu[11], Ariella B. Hanker[12,13], Ganesh V. Raj[9,12], Guanghui Zhu[14,15], Housheng Hansen He[14,15], Zhao Wang[7], Carlos L. Arteaga[12,13], Han Liang[5], Felix Y. Feng[3,16], Yunguan Wang[17], Tao Wang[2,12], Ping Mu[1,12,18†]

Affiliations:

[1.] Department of Molecular Biology, UT Southwestern Medical Center, Dallas, TX 75390, USA

[2.] Quantitative Biomedical Research Center, Peter O'Donnell Jr. School of Public Health, UT Southwestern Medical Center, Dallas, TX, USA, 75390

[3.] Department of Cellular and Molecular Medicine, School of Medicine, University of California San Diego, CA 92093, USA

[4.] Department of Radiation Oncology, University of California, San Francisco, CA 94143, USA

[5.] Department of Bioinformatics and Computational Biology, The University of Texas MD Anderson Cancer Center, Houston, TX 77030, USA

[6.] Department of Biochemistry & Molecular Biology, Louisiana State University Health Shreveport, LA 71103, USA

[7.] Verna and Marrs McLean Department of Biochemistry and Molecular Biology, Baylor College of Medicine, Houston, TX 75390, USA

[8.] Bioinformatics Core Facility of the Lyda Hill Department of Bioinformatics, UT Southwestern Medical Center, Dallas, TX 75390, USA

[9.] Department of Urology, UT Southwestern Medical Center, Dallas, TX 75390, USA

[10.] Human Oncology & Pathogenesis Program, Memorial Sloan Kettering Cancer Center, NYC, NY 10065, USA

[11.] Division of Biostatistics, Department of Public Health Sciences, University of Virginia School of Medicine, Charlottesville, VA 22903, USA

[12.] Department of Internal Medicine, UT Southwestern Medical Center, Dallas, TX 75390, USA

[13.] Harold C. Simmons Comprehensive Cancer Center, UT Southwestern Medical Center, Dallas, TX 75390, USA

[14.] Department of Medical Biophysics, University of Toronto, Toronto, Ontario, Canada

[15.] Princess Margaret Cancer Center, University Health Network, Toronto, Ontario, Canada

[16.]Helen Diller Family Comprehensive Cancer Center, University of California, San Francisco, CA 94143, USA

[17.] Division of Biomedical Informatics, Cincinnati Children's Hospital Medical Center, Cincinnati, OH 45229, USA

[18.] Hamon Center for Regenerative Science and Medicine, UT Southwestern Medical Center, Dallas, TX 75390, USA

† Corresponding Author & Lead Contact

Contents:

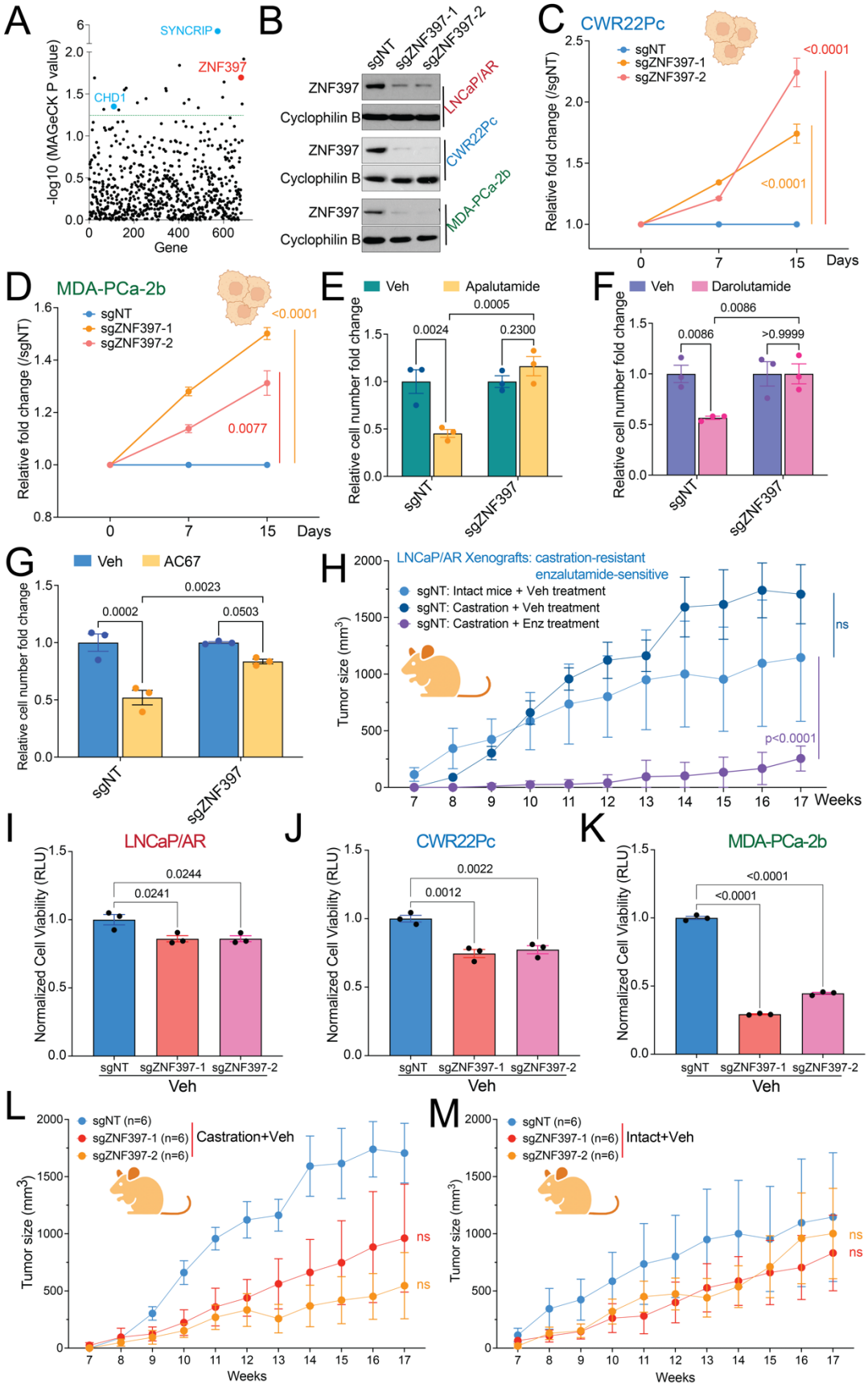
A
SYNCRIP
ZNF397
CHD1
-log10 (MAGeCK P value)
Gene
B
sgNT
sgZNF397-1
sgZNF397-2
ZNF397
Cyclophilin B
LNCaP/AR
CWR22Pc
MDA-PCa-2b
C
CWR22Pc
sgNT
sgZNF397-1
sgZNF397-2
<0.0001
<0.0001
Relative fold change (/sgNT)
Days
D
MDA-PCa-2b
sgNT
sgZNF397-1
sgZNF397-2
<0.0001
0.0077
Relative fold change (/sgNT)
Days
E
Veh
Apalutamide
0.0005
0.0024
0.2300
Relative cell number fold change
sgNT
sgZNF397
F
Veh
Darolutamide
0.0086
0.0086
>0.9999
Relative cell number fold change
sgNT
sgZNF397
G
Veh
AC67
0.0023
0.0002
0.0503
Relative cell number fold change
sgNT
sgZNF397
H
LNCaP/AR Xenografts: castration-resistant
enzalutamide-sensitive
sgNT: Intact mice + Veh treatment
sgNT: Castration + Veh treatment
sgNT: Castration + Enz treatment
ns
p<0.0001
Tumor size (mm3)
Weeks
I
LNCaP/AR
0.0244
0.0241
Normalized Cell Viability (RLU)
sgNT
sgZNF397-1
sgZNF397-2
Veh
J
CWR22Pc
0.0022
0.0012
Normalized Cell Viability (RLU)
sgNT
sgZNF397-1
sgZNF397-2
Veh
K
MDA-PCa-2b
<0.0001
<0.0001
Normalized Cell Viability (RLU)
sgNT
sgZNF397-1
sgZNF397-2
Veh
L
sgNT (n=6)
sgZNF397-1 (n=6)
sgZNF397-2 (n=6)
Castration+Veh
ns
ns
Tumor size (mm3)
Weeks
M
sgNT (n=6)
sgZNF397-1 (n=6)
sgZNF397-2 (n=6)
Intact+Veh
ns
ns
Tumor size (mm3)
Weeks

Figure S1. ZNF397-deficiency has bifurcated effects on PCa with or without AR inhibition. (A) Dot plot represents the results of MAGeCK algorithm-based re-analysis of the *in vivo* library screening. ZNF397 is presented as red dot, CHD1 and SYNCRIP (previously identified top hits) are presented as blue dots. p values were calculated with MAGeCK and green line represents the statistical significance cutoff line ($p<0.05$). (B) Western blot of ZNF397 in a series of human PCa cell lines with CRISPR-based ZNF397-KO. (C) Relative cell number fold change of CWR22Pc cells transduced with Cas9 and annotated CRISPR guide RNAs, measured by FACS-based competition assay. Enz denotes 1μM enzalutamide treatment for 15 days. (D) Relative cell number fold change of MDA-PCa-2b cells transduced with Cas9 and annotated CRISPR guide RNAs, measured by FACS-based competition assay. Enz denotes 10 μM enzalutamide treatment for 15 days. (E) Relative cell number fold change of LNCaP/AR cells transduced with Cas9 and annotated CRISPR guide RNAs. Cells were treated with Vehicle (DMSO) or 5μM Apalutamide for 4 days. (F) Relative cell number fold change of LNCaP/AR cells transduced with Cas9 and annotated CRISPR guide RNAs. Cells were treated with Vehicle (DMSO) or 30μM Darolutamide for 4 days. (G) Relative cell number fold change of LNCaP/AR cells transduced with Cas9 and annotated CRISPR guide RNAs. Cells were treated with Vehicle (DMSO) or 80nM AR PROTAC AC67 for 4 days. (H) Tumor growth curve of xenografted wildtype LNCaP/AR cells treated with annotated conditions. Veh denotes 0.5% CMC + 0.1% Tween 80. Number of tumors in each group were annotated. (I-K) Bar plots represent the relative cell viability of LNCaP/AR (I), CWR22Pc (J), and MDA-PCa-2b cells (K) transduced with Cas9 and annotated CRISPR guide RNAs and treated with vehicle (Veh), measured as values of relative luminescence units (RLU) and normalized to sgNT. Veh denotes DMSO. (L) Tumor growth curve of xenografted LNCaP/AR cells transduced with annotated guide RNAs in castrated mice treated with vehicle. Veh denotes 0.5% CMC + 0.1% Tween 80. Number of tumors in each group were annotated. (M) Tumor growth curve of xenografted LNCaP/AR cells transduced with annotated guide RNAs in intact mice treated with vehicle. Veh denotes 0.5% CMC + 0.1% Tween 80. Number of tumors in each group were annotated. For all panels unless otherwise noted, mean ± s.e.m. is presented and p values were calculated using two-way ANOVA with Bonferroni multiple-comparison test. Schematic figure was created with BioRender.com.

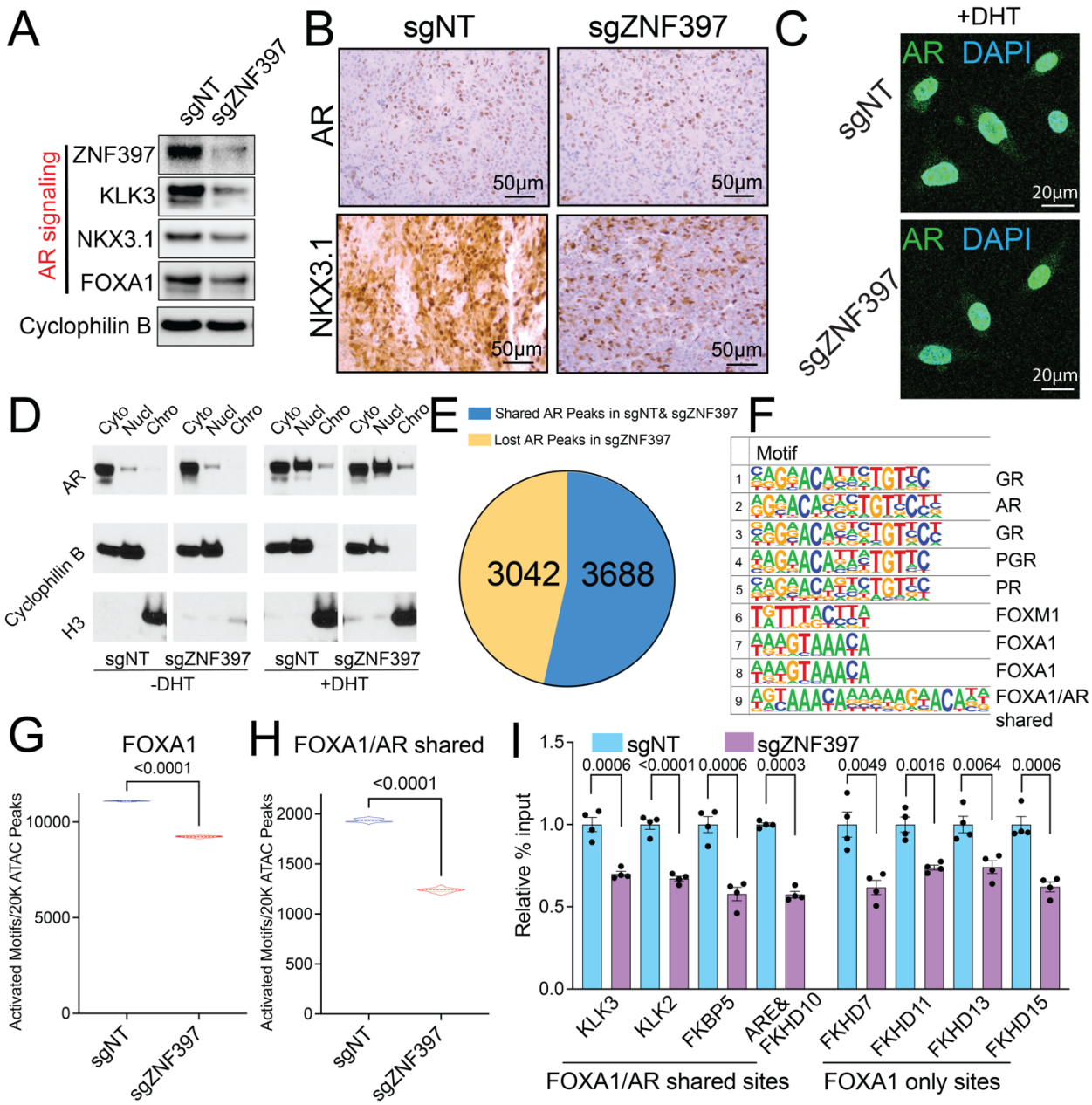

Figure S2. The impact of ZNF397-deficiency on AR protein and AR cistrome.
(A) Western blots represent canonical AR target proteins in sgNT and sgZNF397 LNCaP/AR cells. (B) IHC staining for AR and AR target protein NKX3.1 in sgNT and sgZNF397 xenograft tumor slides. A scale bar represents 50 μm. (C) Representative IF staining for AR in LNCaP/AR cells transduced with Cas9 and annotated guide RNAs. (D) Western blots represent the levels of AR protein in the cytoplasmic, nuclear-soluble, and chromatin-bound fractions from annotated cells. Cyto denotes cytoplasmic, nucl denotes nuclear and chro denotes chromatin. Histone H3 (chromatin) and cyclophilin B (cytoplasmic and nuclear) served as fractionation controls. (E) A pie chart illustrates the number of shared and depleted AR binding peaks in ZNF397-KO cells compared to wildtype cells, as determined by AR ChIP-Seq. (F) Motif enrichment analysis reveals the most significantly lost motifs in ZNF397-KO cells, with the transcription factors binding to the corresponding motifs annotated on the right. (G) A violin plot displays the number of enriched

FOXA1 motif peaks per 20k ATAC-Seq peaks in annotated cells and treatment conditions. (H) A violin plot displays the number of enriched FOXA1 and AR shared motif peaks per 20k ATAC-Seq peaks in annotated cells and treatment conditions. p values were calculated using a two-tailed t-test. (I) FOXA1 ChIP-qPCR results for canonical FOXA1 only sites and AR/FOXA1 shared sites in LNCaP/AR cells transduced with annotated constructs. For all panels, unless otherwise noted, the mean ± s.e.m. is presented, and p values were calculated using two-way ANOVA with Bonferroni multiple-comparison test.

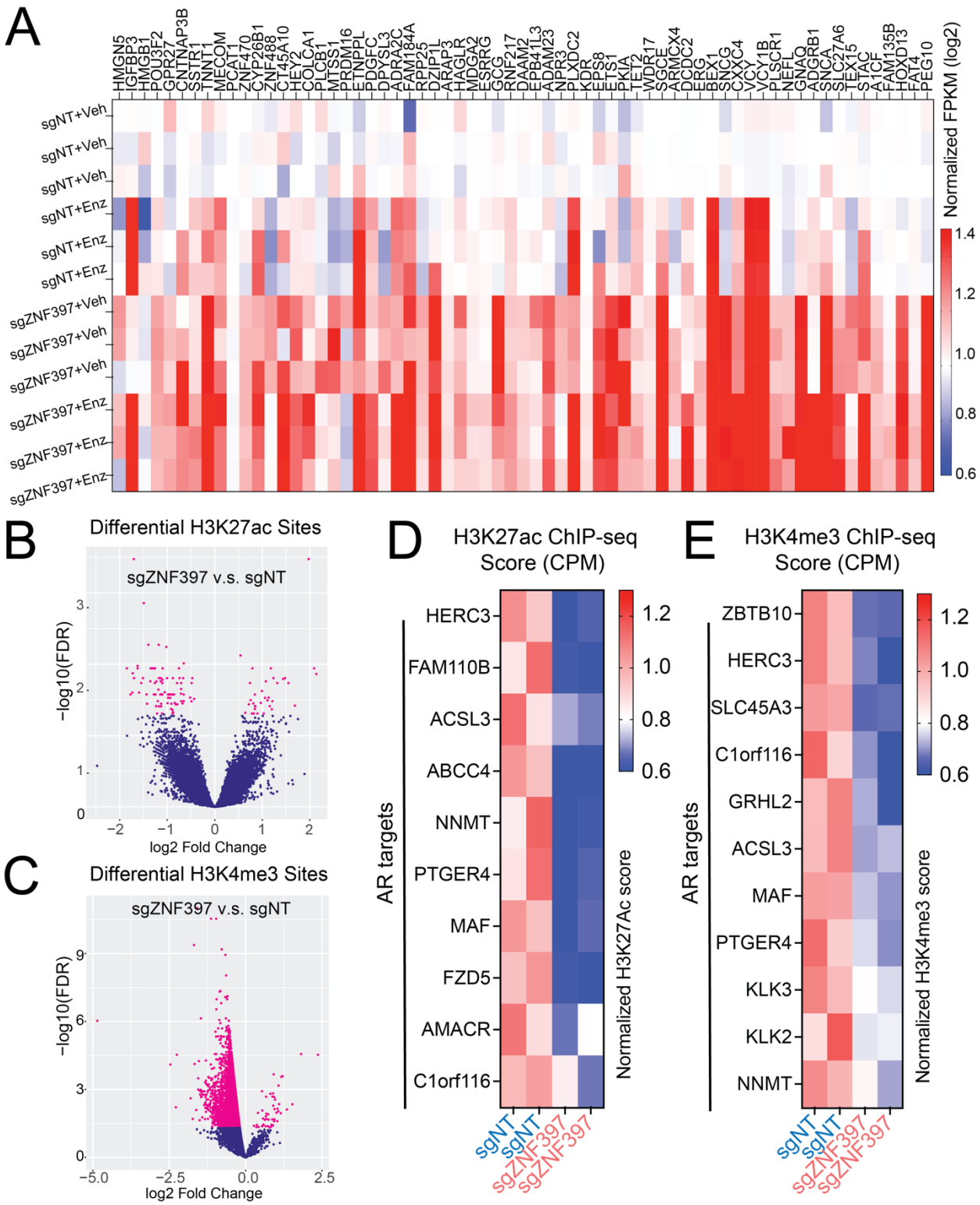

Figure S3. ZNF397 is required for the activation of canonical AR transcriptional program. (A) Heatmap represents the most significantly upregulated genes in ZNF397-KO cells compared to the control cells. (B) Volcano plot represents the genomic loci depleted or gained H3K27ac peaks, in ZNF397-KO cells compared to the control cells. Significantly changed gene loci were annotated as pink dots. (C) Volcano plot represents the genomic loci with depleted or gained

H3K4me3 peaks, in ZNF397-KO cells compared to the control cells. Significantly changed gene loci were annotated as pink dots. (D) Heatmap represents the H3K27ac enrichment score (CPM, see Methods) in the genomic loci of AR Score genes in the sgZNF397 cells compared to sgNT cells. (E) Heatmap represents the H3K4me3 enrichment score (CPM, see Methods) in the genomic loci of AR Score genes in the sgZNF397 cells compared to sgNT cells. For all panels unless otherwise noted, reads from two independent cell cultures/guide were plotted, matching input controls were used for analysis.

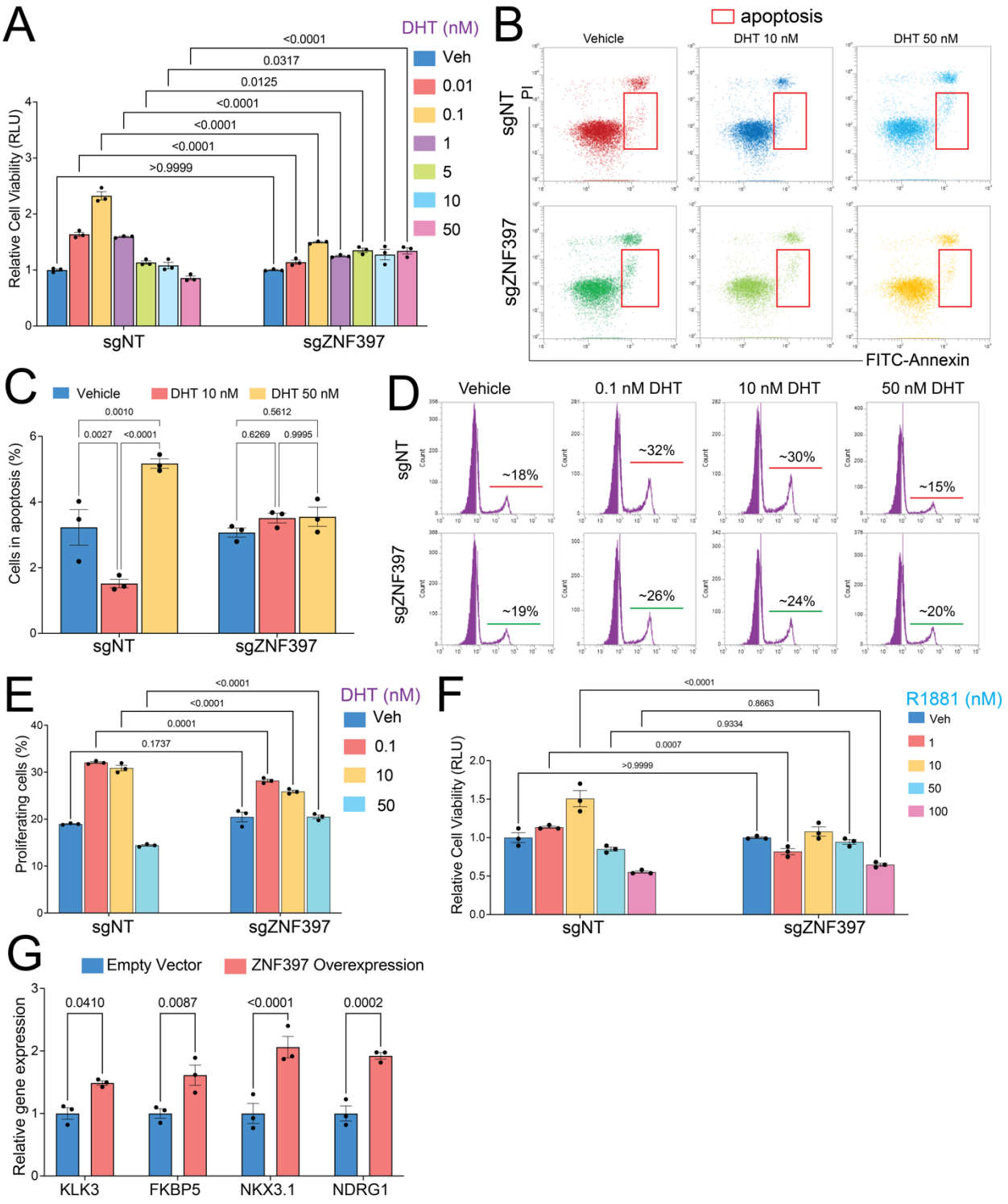

Figure S4. ZNF397-KO impairs DHT-induced AR signaling activation.
(A) Bar plot represents the relative cell viability of LNCaP/AR cells transduced with annotated guide RNAs and treated with different doses of DHT for 7 days, measured as values of relative luminescence units (RLU) and normalized to vehicle-treated conditions. (B) Representative FACS results showing the percentage of apoptotic LNCaP/AR cells transduced with annotated guide

RNAs under annotated concentration of DHT-treatments, measured by a FACS-based Annexin-PI apoptosis assay. (C) Bar plots represent the quantification of panel B, displaying the percentage of apoptotic cells under annotated concentration of DHT-treatments. (D) Representative FACS results showing the percentage of activated proliferating LNCaP/AR cells transduced with annotated hairpins under annotated concentration of DHT-treatments, measured by a FACS-based EdU-incorporation assay. (E) Bar plots represent the quantification of panel D, displaying the percentage of EdU-positive and actively proliferating cells under annotated conditions. (F) Bar plot representing the relative cell viability of LNCaP/AR cells transduced with annotated guide RNAs and treated with different doses of R1881 for 4 days, measured as values of relative luminescence units (RLU) and normalized to vehicle-treated conditions. (G) Relative gene expression levels of canonical AR target genes in the LNCaP/AR cells transduced with empty or ZNF397 overexpression constructs, measured by qPCR assay. Data are normalized to the average expression in empty-vector transduced cells. For all panels unless otherwise noted, n=3 independently treated cell cultures and mean ± s.e.m. is presented. p values were calculated using two-way ANOVA with Bonferroni multiple-comparison test.

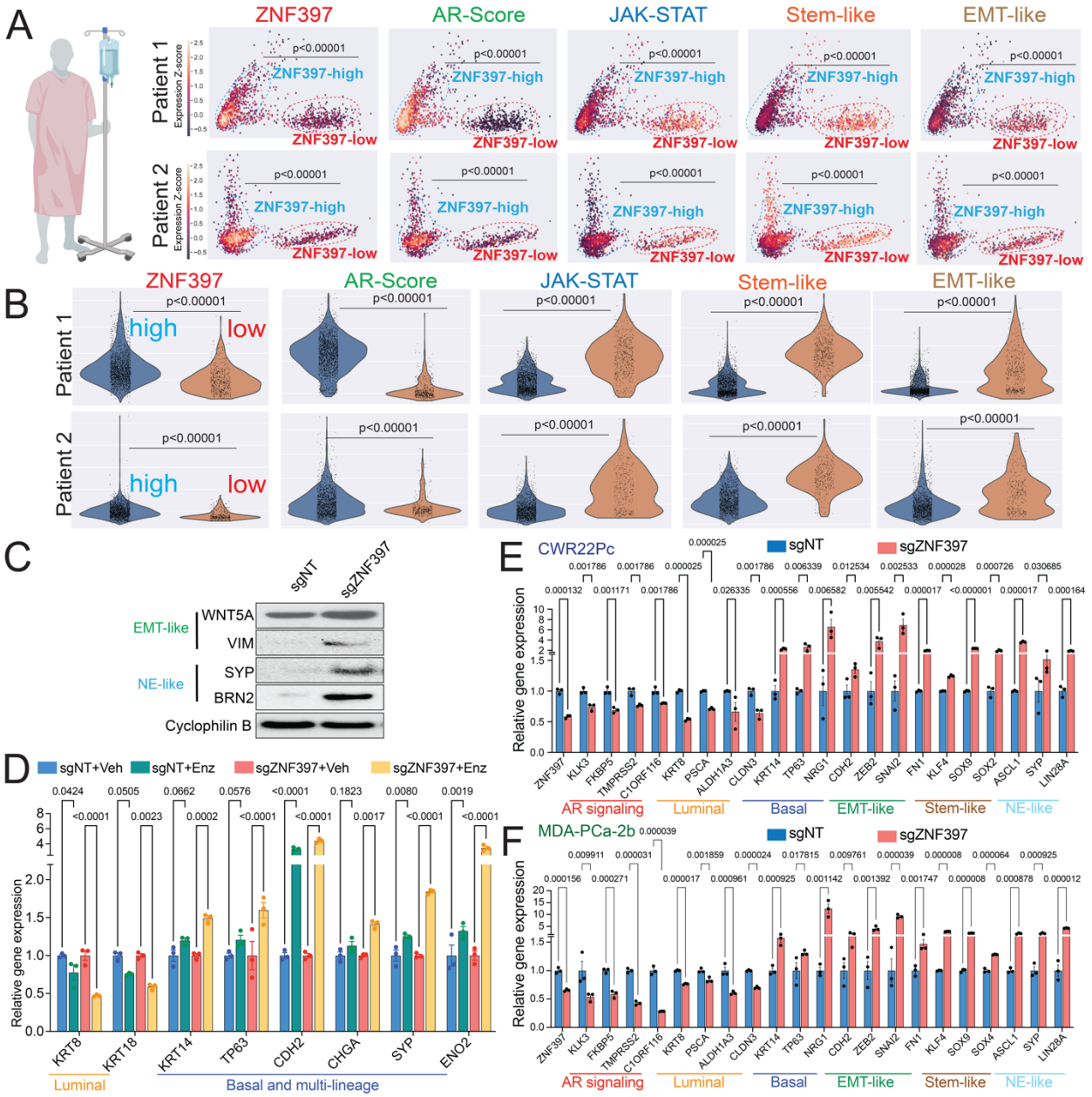

Figure S5. ZNF397-KO promotes multilineage and lineage plastic gene expression.
(A) Principal-component analysis (PCA) plots of two human CRPC biopsy samples (3, 53). For each sample, single cell transcriptomic profiles are colored by the expression (Log2CPM) of lineage gene signatures. (B) Violin plots represent the expression scores of lineage gene signatures in subclones with high vs low ZNF397 expression in both CRPC patient. p-values were calculated by Mann-Whitney U test. (C) Western blots represent lineage-specific marker proteins in sgNT and sgZNF397 LNCaP/AR cells, from the same western blot experiment as Fig.S2A. (D) Relative gene expressions of lineage marker genes in LNCaP/AR cells transduced with Cas9 and annotated guide RNAs, and treated with vehicle (Veh, DMSO) or enzalutamide (Enz, 10 μM) for 7 days, normalized and compared to Veh group. (E) Relative gene expression levels of canonical lineage specific marker genes in the CWR22Pc cells transduced with Cas9 and annotated guide RNAs, measured by qPCR assay, normalized to sgNT cells. (F) Relative gene expression levels of

canonical lineage specific marker genes in the MDA-PCa-2b cells transduced with Cas9 and annotated guide RNAs, measured by qPCR assay, normalized to sgNT cells. For all panels , n=3 independently treated cell cultures and mean ± s.e.m. is presented. p values were calculated using two-way ANOVA with Bonferroni multiple-comparison test. Schematic figure was created with BioRender.com.

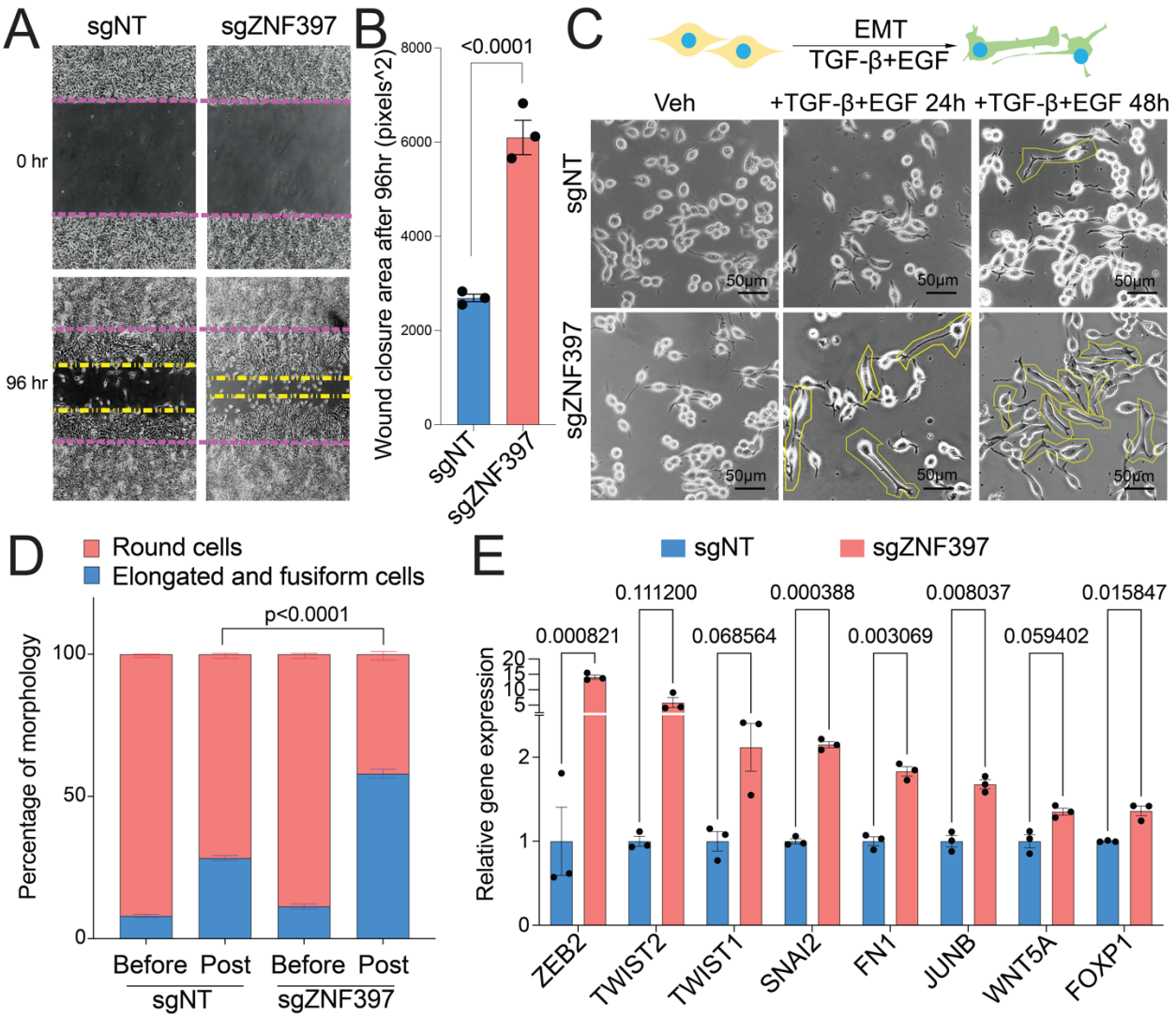

Figure S6. ZNF397-KO promotes stem-like and EMT-like transcriptional programs.
(A) Representative images of an LNCaP/AR cell wound healing assay from three independently treated cell cultures. (B) Quantification of the occupied areas of invading cells from three representative images, taken from three independently treated cell cultures for each of the cell lines. (C) Representative images show the morphological changes in annotated LNCaP/AR cells treated with TGF-β + EGF, derived from three independently treated cell cultures. (D) Quantification of the percentage of "elongated and fusiform" cells from three representative images, taken from three independently treated cell cultures for each cell line. p value was calculated with Fisher's Exact Test. (E) Relative gene expression levels of EMT-like lineage marker genes in LNCaP/AR cells transduced with Cas9 and annotated guide RNAs, normalized to sgNT group. For all panels unless otherwise noted, n=3 independently treated cell cultures and mean ± s.e.m. is presented. p values were calculated using multiple t-test with Benjamini correction.

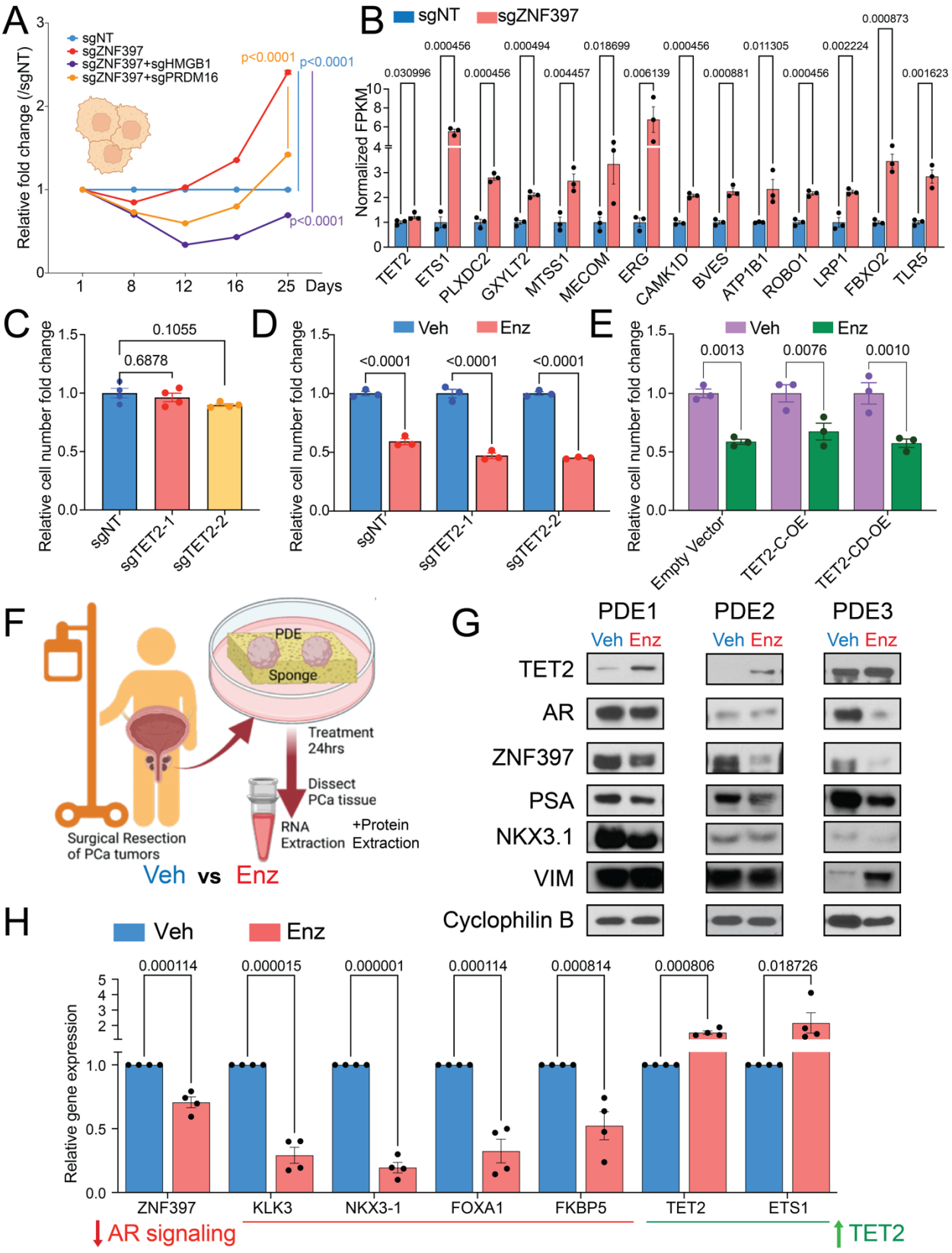

Figure S7. ZNF397-KO led to induction of TET2 downstream genes.

(A) Relative cell number fold change of LNCaP/AR cells transduced with Cas9 and annotated CRISPR guide RNAs, measured by FACS-based competition assay. Enz denotes 10 μM enzalutamide treatment for 25 days. (B) Relative gene expression levels of canonical TET2 target genes in the LNCaP/AR cells transduced with Cas9 and annotated guide RNAs, measured by RNA-seq analysis, normalized to sgNT cells. (C) Relative cell number fold change of LNCaP/AR cells transduced with Cas9 and annotated CRISPR guide RNAs and treated with vehicle. p values were calculated using one-way ANOVA with Bonferroni multiple-comparison test. (D) Relative cell number fold change of LNCaP/AR cells transduced with Cas9 and annotated CRISPR guide RNAs and treated with vehicle or enzalutamide. (E) Relative cell number fold change of LNCaP/AR cells transduced with annotated constructs expressing truncated version of TET2 and treated with vehicle or enzalutamide. C: cysteine-rich domain of TET2; CD: catalytic domain of TET2. (F) Schematic figure represents the establishment of patient-derived explant (PDE) models treated with vehicle or 10 μM enzalutamide for 24 hours. (G) Western blots represent the protein levels of ZNF397, AR, TET2 and lineage markers in independent PDEs (n=3) treated with vehicle (Veh) or enzalutamide (Enz). (H) Relative gene expression of ZNF397, AR pathway and TET2 target in PDEs (n=4) treated with vehicle (Veh) or enzalutamide (Enz). For all panels unless otherwise noted, n = 3 independently treated cell cultures and mean ± s.e.m. is presented. p values were calculated using multiple t-tests with Benjamini correction. Schematic figure was created with BioRender.com.

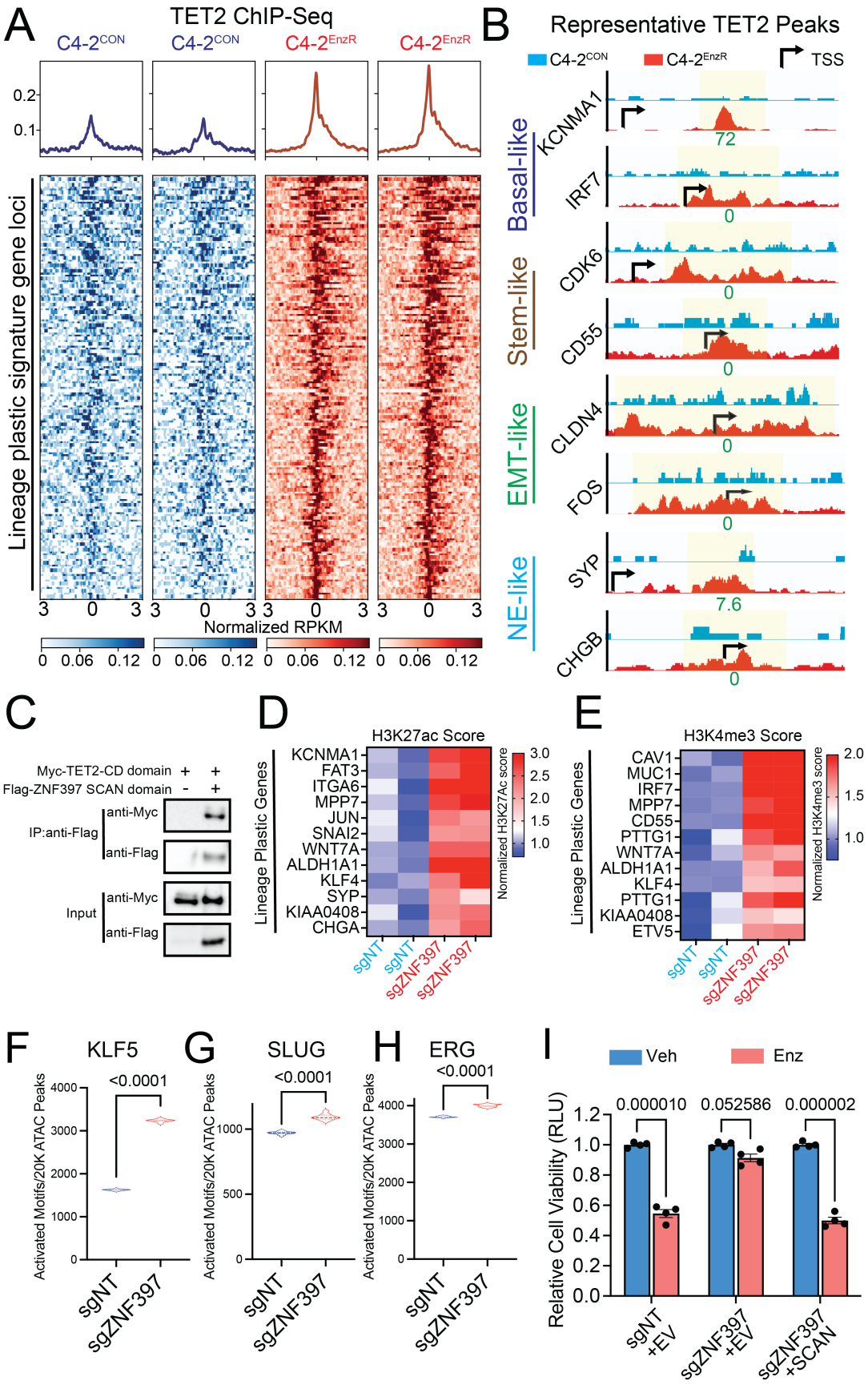
A
TET2 ChIP-Seq
C4-2CON
C4-2CON
C4-2EnzR
C4-2EnzR
0.2
0.1
Lineage plastic signature gene loci
3 0 3
Normalized RPKM
0 0.06 0.12
B
Representative TET2 Peaks
C4-2CON
C4-2EnzR
TSS
Basal-like
KCNMA1
72
IRF7
0
Stem-like
CDK6
0
CD55
0
EMT-like
CLDN4
0
FOS
0
NE-like
SYP
7.6
CHGB
0
C
Myc-TET2-CD domain + +
Flag-ZNF397 SCAN domain - +
IP:anti-Flag
anti-Myc
anti-Flag
Input
anti-Myc
anti-Flag
D
H3K27ac Score
Lineage Plastic Genes
KCNMA1
FAT3
ITGA6
MPP7
JUN
SNAI2
WNT7A
ALDH1A1
KLF4
SYP
KIAA0408
CHGA
Normalized H3K27Ac score
3.0
2.5
2.0
1.5
1.0
sgNT
sgNT
sgZNF397
sgZNF397
E
H3K4me3 Score
Lineage Plastic Genes
CAV1
MUC1
IRF7
MPP7
CD55
PTTG1
WNT7A
ALDH1A1
KLF4
PTTG1
KIAA0408
ETV5
Normalized H3K4me3 score
2.0
1.5
1.0
sgNT
sgNT
sgZNF397
sgZNF397
F
KLF5
<0.0001
Activated Motifs/20K ATAC Peaks
4000
3000
2000
1000
0
sgNT
sgZNF397
G
SLUG
<0.0001
Activated Motifs/20K ATAC Peaks
1000
500
0
sgNT
sgZNF397
H
ERG
<0.0001
Activated Motifs/20K ATAC Peaks
4000
3000
2000
1000
0
sgNT
sgZNF397
I
Veh
Enz
0.000010
0.052586
0.000002
Relative Cell Viability (RLU)
1.2
1.0
0.8
0.6
0.4
0.2
0.0
sgNT +EV
sgZNF397 +EV
sgZNF397 +SCAN

Figure S8. ZNF397-KO promotes transcriptional activation of TET2 downstream genes.
(A) Distribution of TET2 binding peaks on canonical lineage plastic and multilineage gene signatures based on TET2 ChIP-seq results in LNCaP derived C4-2 cells (59). (B) Representative TET2 binding sites in the genomic loci of canonical lineage plastic signature genes in the C4-$2^{Enz\text{-}R}$ vs C4-2^{CON} cells, based on TET2 ChIP-seq analysis. The binding peak distances (kilo base pair) to TSS (Transcriptional Start Site) are annotated in green. (C) Co-immunoprecipitation (Co-IP) of ZNF397 and the TET2 CD domain with a Flag or Myc tag in HEK293T cells. (D) Heatmap represents the H3K27ac enrichment score (CPM, see Methods) in the genomic loci of lineage-specific signature genes in the sgZNF397 cells compared to sgNT cells. (E) Heatmap represents the H3K4me3 enrichment score (CPM, see Methods) in the genomic loci of lineage-specific signature genes in the sgZNF397 cells compared to sgNT cells. (F-H) Violin plot represents the number of peaks belongs to motifs known to be correlated with enhanced TET2 activity: (F) KLF5 motif, (G) SLUG motif, (H) ERG motif, per 20k ATAC-Seq peaks in annotated cells and treatment conditions. n = 3 independently treated cell cultures were used for the triplicates in ATAC-Seq and mean ± s.e.m. is presented. p values were calculated using two-tailed t-test. (I) Bar plots represent the relative cell viability of LNCaP/AR cells transduced with annotated CRISPR guide RNAs and rescue construct expressing ZNF397 SCAN domain, measured as values of relative luminescence unit (RLU) and normalized to vehicle treated conditions. Enz denotes 10 μM enzalutamide treatment for 7 days and Veh denotes DMSO.

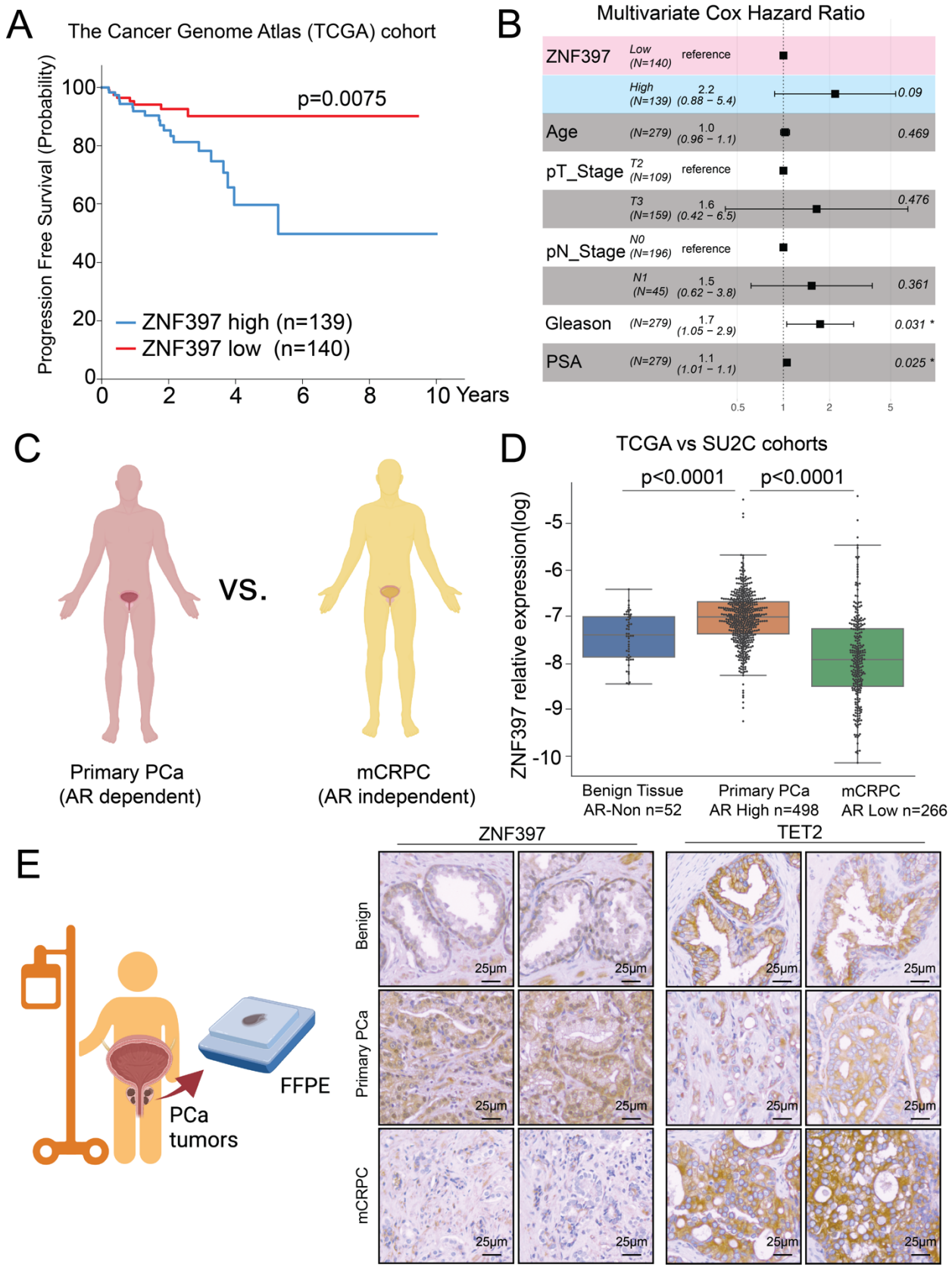
A
The Cancer Genome Atlas (TCGA) cohort
Progression Free Survival (Probability)
p=0.0075
ZNF397 high (n=139)
ZNF397 low (n=140)
Years
B
Multivariate Cox Hazard Ratio
ZNF397
Low (N=140) reference
High (N=139) 2.2 (0.88 – 5.4) 0.09
Age (N=279) 1.0 (0.96 – 1.1) 0.469
pT_Stage
T2 (N=109) reference
T3 (N=159) 1.6 (0.42 – 6.5) 0.476
pN_Stage
N0 (N=196) reference
N1 (N=45) 1.5 (0.62 – 3.8) 0.361
Gleason (N=279) 1.7 (1.05 – 2.9) 0.031 *
PSA (N=279) 1.1 (1.01 – 1.1) 0.025 *
C
vs.
Primary PCa
(AR dependent)
mCRPC
(AR independent)
D
TCGA vs SU2C cohorts
p<0.0001
p<0.0001
ZNF397 relative expression(log)
Benign Tissue
AR-Non n=52
Primary PCa
AR High n=498
mCRPC
AR Low n=266
E
FFPE
PCa
tumors
ZNF397
TET2
Benign
Primary PCa
mCRPC
25μm

Figure S9. ZNF397-deficiency has bifurcated effects on AR-dependent vs AR-independent PCas.
(A) Kaplan-Meier curves represent the progression-free survival of primary PCa patients with high (above median) or low (below median) expression of ZNF397 in TCGA cohort. The p-value was calculated using the log-rank test. (B) Multivariate Cox hazard ratio analysis represents the significant risk factors associated with disease progression in TCGA patient cohort. The p value was calculated with the log-rank test. (C, D) Box plots represent the relative expression of ZNF397 in patients with solid normal tissue, primary tumor, and mCRPC tumor in the TCGA and SU2C cohorts, respectively. p-values were calculated using the Kruskal-Wallis test with Benjamini correction. (E) Representative IHC staining for ZNF397 and TET2 proteins on FFPE slides of solid normal tissue, primary tumor, and mCRPC tumor. A scale bar represents 25 μm. All schematic figure was created with BioRender.com.

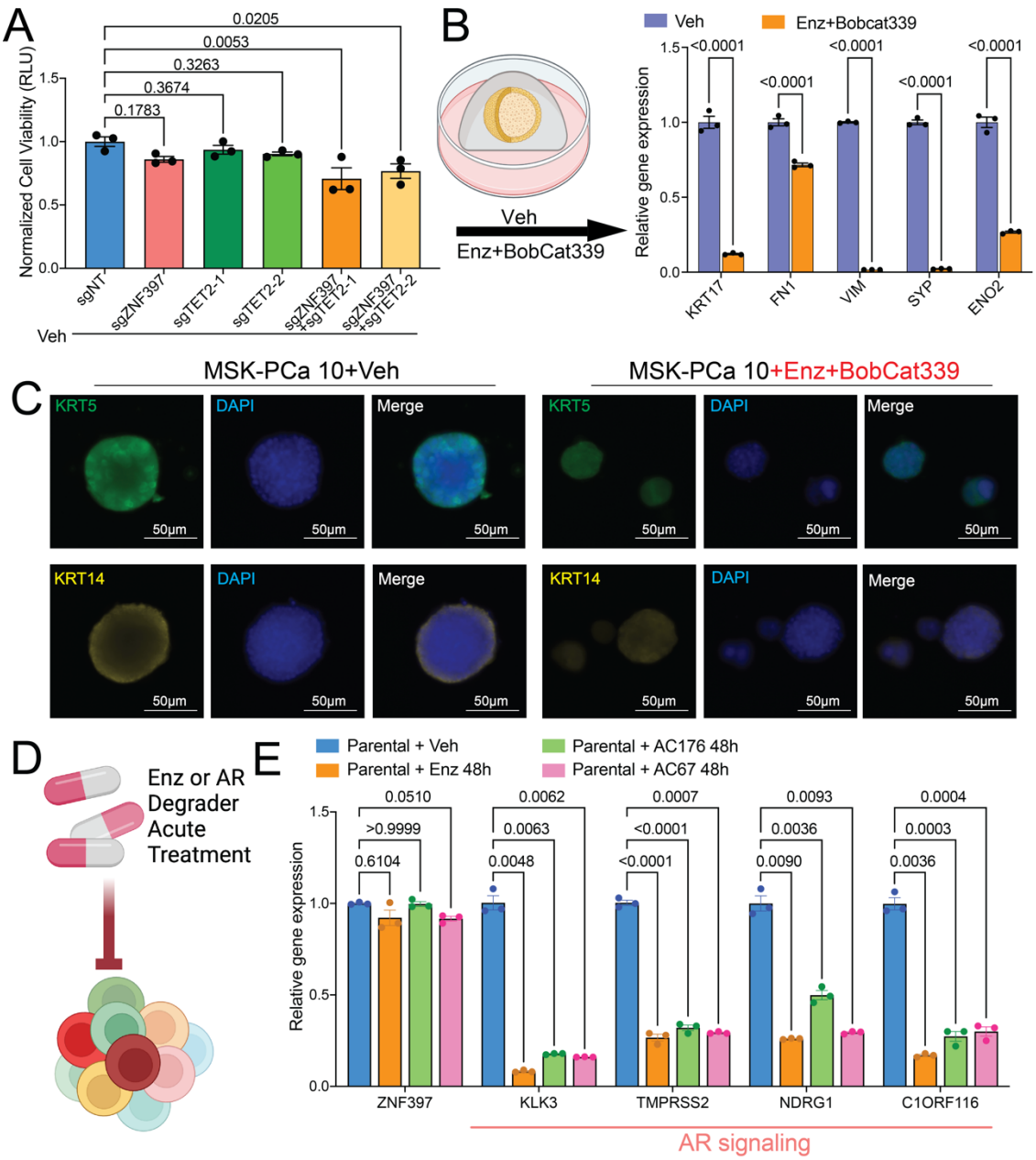

Figure S10. Targeting TET2-driven epigenetic rewiring to overcome resistance.
(A) Bar plots represent the relative cell viability of LNCaP/AR cells transduced with Cas9 and annotated CRISPR guide RNAs, measured as values of relative luminescence unit (RLU) and normalized to sgNT. (B) Relative gene expression of lineage plasticity marker genes in MSK-PCa10 treated with enzalutamide (Enz) and Bobcat339 (Bobcat). (C) IF staining for lineage plasticity markers in MSK-PCa10 treated with enzalutamide (Enz) and Bobcat339 (Bobcat), with representative images shown from n=3 independently treated cell cultures. (D) Schematic representation of acute AR inhibition using enzalutamide and AR degraders. (E) Relative gene expression of ZNF397 versus AR target genes in parental LNCaP/AR cells treated with enzalutamide (Enz) or two AR degraders (AC67 and AC176) for 48 hours, normalized to sgNT+Veh. For all panels, unless otherwise noted, n = 3 independently treated cell cultures and

mean ± s.e.m. is presented. p values were calculated using two-way ANOVA with Bonferroni multiple-comparison test. Schematic figure was created with BioRender.com.

Supplemental Table Legends:

Table S1. Significantly Altered AR ChIP-seq Peaks in ZNF397-KO Cells
Table S2. Differentially Expressed Genes in ZNF397-KO Cells
Table S3. Significantly Enriched or Depleted Signaling Pathways in GSEA Analysis
Table S4. Candidate Resistance Driver Genes in ZNF397-KO Cells
Table S5. Lineage-Specific and AR Target Gene Signatures
Table S6. Key Resources